JOURNAL OF VIROLOGY, Apr. 2005, p. 4755–4763 Vol. 79, No. 8
0022-538X/05/$08.00+0 doi:10.1128/JVI.79.8.4755–4763.2005

Visualization and Characterization of the Intracellular Movement of Vaccinia Virus Intracellular Mature Virions

Brian M. Ward*

Department of Microbiology and Immunology, University of Rochester Medical Center, Rochester, New York

Received 16 August 2004/Accepted 23 November 2004

Previous work indicated that vaccinia intracellular mature virus (IMV) utilizes microtubules to move from the viral factory to the site of intracellular envelopment and that expression of the viral A27 protein is required for this transport. To investigate further the role of A27 in IMV intracellular transport, a recombinant vaccinia virus was constructed that had the A27L gene deleted and expressed a yellow fluorescent protein (YFP)-A4 chimera in place of the normal A4 protein. The resulting recombinant, vYFP-A4/ΔA27, produced relatively normal quantities of virus in a one-step growth curve but had a small plaque phenotype. Subsequent experiments demonstrated that vYFP-A4/ΔA27 was severely defective in envelope virus production. Despite the absence of A27, live digital video fluorescent microscopy visualized YFP-labeled IMV movement in cells infected with the recombinant. Virion movement approached 3 μm/s and was sensitive to the microtubule depolymerizing drug nocodazole. In addition, IMV could be discerned transiting away from and back towards viral factories. Immunofluorescent staining determined that the distance traveled by A27-deficient virions was sufficient for transport to the site of envelopment. These results indicate that IMVs are capable of bidirectional movement on microtubules, suggesting that they are able to interact with both kinesin and dynein microtubule motors in the absence of A27 and that the distance traveled is sufficient to deliver IMV to the site of wrapping.

Vaccinia virus replicates entirely in the cytoplasm and produces both intracellular and extracellular forms of infectious virions. Virion production occurs in a discrete area of the cytoplasm termed the viral factory (21). Intracellular mature virus (IMV) is the first infectious form produced in the viral factory (8, 15). A subset of IMVs are transported away from the viral factory to the sight of wrapping in the juxta-nuclear region where they are enveloped by an extra double membrane derived from the trans-Golgi network or endosomal cisternae (29, 31) to become intracellular enveloped virions (IEV). IEV interact with cellular kinesin through the viral A36 protein and are transported via microtubules from the site of wrapping to the cell periphery, where the outermost IEV membrane fuses with the plasma membrane depositing cell-associated enveloped virus (CEV) on the cell surface (13, 18, 23, 34–36). Actin polymerization occurs directly beneath the CEV on the cytosolic side of the membrane to produce actin tails that propel CEV away from the cell. Enveloped virions are eventually released from the cell surface and are called extracellular enveloped virions (EEV) (3, 7, 16, 30). While IMVs make up the majority of progeny virions, the enveloped forms of the virus, CEV and EEV, are believed to be critical for cell-to-cell and long-range spread because mutations that decrease enveloped virus production result in a small plaque phenotype (1, 3, 4, 22).

(Vaccinia virus open reading frames are designated by a capital letter indicating a HindIII restriction endonuclease fragment, a number indicating the position in the HindIII fragment, and a letter [L or R] indicating the direction of transcription, e.g., A27L. The corresponding protein is designated by a capital letter and number, e.g., A27.)

The viral A27 protein has been implicated in various aspects of poxvirus infection and has been predicted to play an important role in virus-cell interaction (9). A27 forms homotrimers and is targeted to the surface of IMV by interacting with A17 where it is the target of neutralizing antibodies (19, 20, 24–26). A role in virus attachment to cells has been proposed due to its ability to bind heparin sulfate (6). A27 is also believed to be involved in virus-to-cell fusion and consequently has been predicted to be the fusion protein for poxvirus entry (10, 14, 25, 26). In addition to being involved in entry, A27 is required for enveloped virus production because repression of its expression or deletion of the first 29 residues reduces EEV production (27, 32). Furthermore, it has been reported that the repression of A27 caused an inhibition of IMV intracellular dissemination, and it was theorized that A27 was required for IMV intracellular virion movement along microtubules (28).

We were interested in studying IMV intracellular movement. Specifically we were interested in which IMV protein interacted with the microtubule motor kinesin and, based on the report of Sanderson et al., thought A27 was a good candidate. A recent report employed the yeast two-hybrid assay to show that the IEV-specific protein A36 interacted with kinesin (34). Utilizing a similar approach we were unable to detect an interaction between A27 and kinesin. To further investigate the role of A27 in IMV movement we constructed a recombinant vaccinia virus that had the entire A27L gene deleted. In this report we show that in the absence of A27, yellow fluorescent protein (YFP)-labeled IMVs were still motile in the cell with speeds approaching 3 μm/s. The movement was bidirectional to and from the viral factory and reversibly inhibited by the microtubule depolymerizing drug nocodazole. Based on

* Corresponding author. Mailing Address: 601 Elmwood Ave., Box 672, Rochester, NY 14642. Phone: (585) 275-9715. Fax: (585) 473-9573. E-mail: Brian_Ward@urmc.rochester.edu.

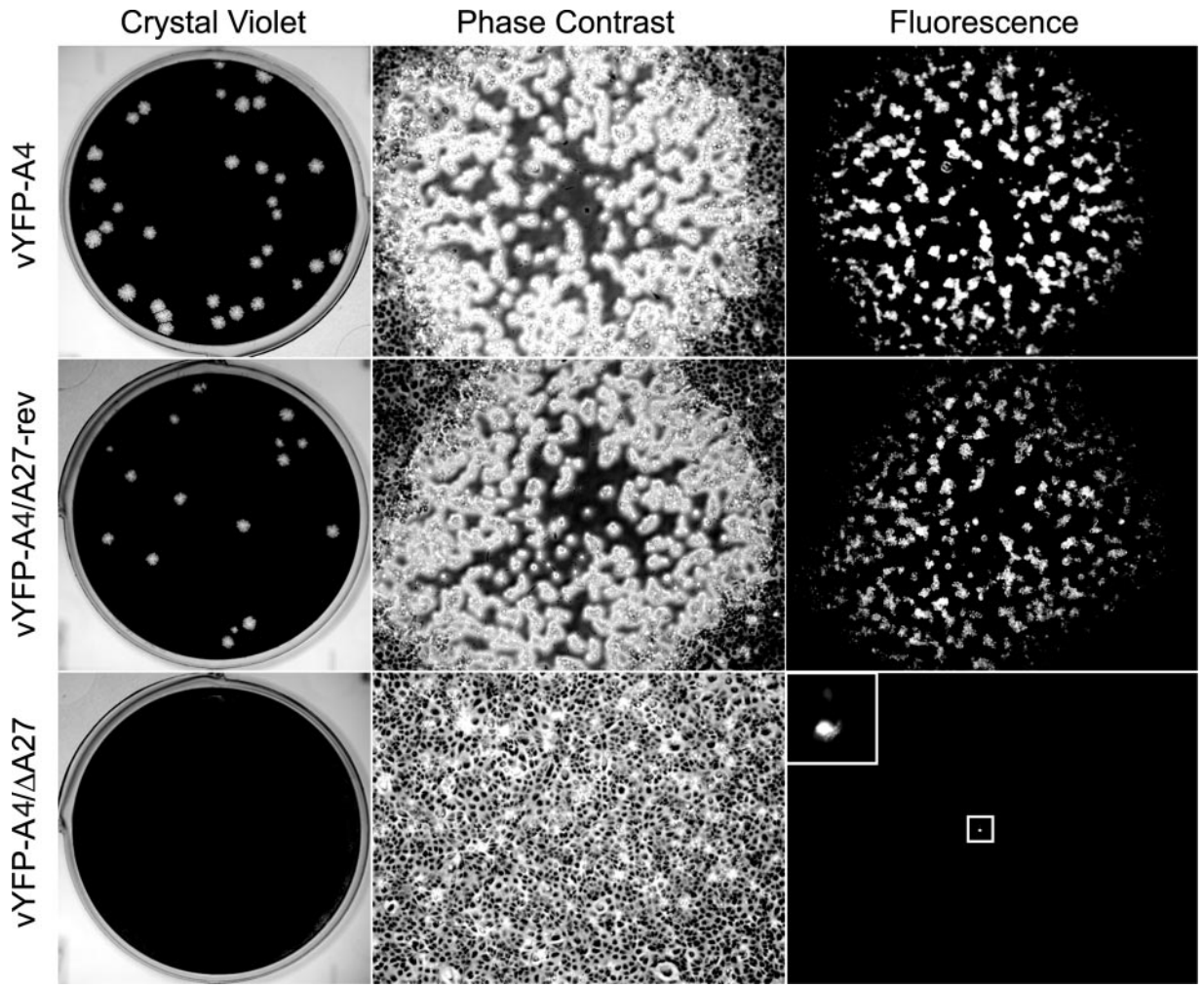

FIG. 1. Plaque phenotypes. The indicated viruses were plated on a monolayer of BS-C-1 cells. After 4 days, plaques were imaged using phase-contrast and fluorescence microscopy. After imaging, cells were stained with crystal violet. The boxed area in the lower right panel is enlarged in order to more clearly show the fluorescing cell.

these results we conclude that A27 is not required for microtubule-dependent movement of IMV.

MATERIALS AND METHODS

Cells and viruses. HeLa and RK13 cell monolayers were grown in Dulbecco's modified Eagle's medium and BS-C-1 cells were grown in Earl's minimum essential medium both supplemented with 10% fetal bovine serum. All viruses were derived from the WR strain of vaccinia virus. Standard procedures were used for the propagation and titration of vaccinia virus (11).

Construction of viruses. CAAGCTTCATCGGTTCGATATGACAAAA and AAGATCTATTTAAAGTACAGATTTTAGAAACTG were used to amplify the left flank of A27L and to add a HindIII and BglII site (underlined), respectively. Similarly, primer pairs CAGATCTGTTCAGACTGGACGGCGC and CGTCGACTTATCATTGCTCGTTATCTCA were used to amplify the right flank of A27L and to add a BglII and SalI site (underlined), respectively. Amplified fragments were cloned into pGEM-T (Promega) and sequenced and excised by digestion with either HindIII/BglII for the left flank or SalI/BglII for the right flank. Excised flanks were cloned into pBMW118/gptrfp that had been cleaved with HindIII-XhoI and resulted in plasmid pBMW109gptrfp. Recombination was used to insert the left and right flanks of A27L into the original locus and subsequently remove the A27L coding sequence. The parental vYFP-A4 recombinant virus and plasmid pSC11 were kind gifts of B. Moss and T. Senkevich. The new recombinant virus was isolated by transient dominant selection, essentially as described previously (35). HeLa cells were infected at a multiplicity of 0.05 with vYFP-A4 and transfected 2 h later with pBMW109gptrfp. After 2 days, cells were harvested, frozen and thawed three times, and used to infect BS-C-1 cells that were treated with mycophenolic acid (MPA), xanthine, and hypoxanthine at concentrations of 25, 250, and 15 μg per ml, respectively. Recombinant viruses that resulted from a single crossover would have the entire plasmid integrated into the viral genome and consequently would be resistant to MPA and would cause cells that are infected with them to fluoresce red. MPA-resistant, red fluorescent cells were picked and their resulting viruses were plaque purified two more times in the presence of MPA before three more picks in the absence of MPA to obtain the desired double-crossover mutant. PCR amplification and sequencing were used to confirm the insertion of the linked flanks and removal of the A27L gene.

Primers CGGATCCTACCAAATATAAATAACGCAGAG and GAGATCT TTTAATTAACAAAAGAGTTAAG were used to amplify the A27L gene along with 50 nucleotides of upstream sequence and to add a BamHI and BglII site (underlined), respectively. The amplified fragment was ligated into pGEM-T and sequenced. Afterwards it was excised with BamHI and BglII and ligated into pSC11 that had been digested with BglII to give pBMW112-SC11. Recombination was used to insert the A27L gene along with its promoter into the thymidine kinase locus. Briefly, HeLa cells were infected with vYFP-A4/ΔA27 and transfection with pBMW112-SC11. The resulting revertant virus vYFP-A4/A27-rev was isolated based on its rescue of the small plaque phenotype and plaque purified on BS-C-1 cells three more times. Insertion of A27L along with its promoter into the thymidine kinase locus was confirmed by PCR and sequencing.

Plaque assay. For plaque assays, BS-C-1 cells were infected using standard protocols and maintained in media containing methylcellulose (11). After 4 days,

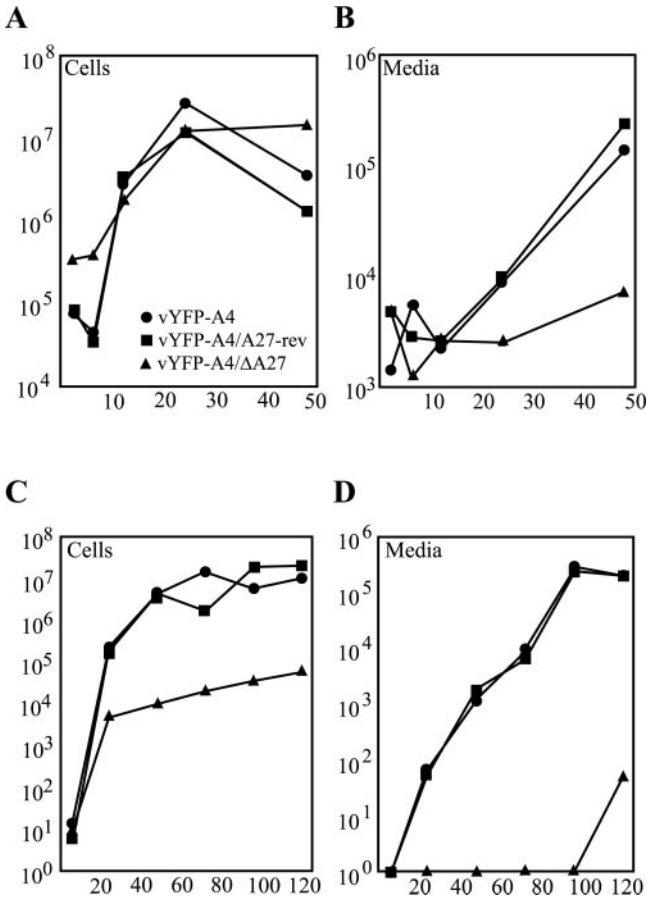

FIG. 2. Virus replication. BS-C-1 cells were infected with either 5 PFU (A and B) or 0.01 PFU (C and D) of the indicated viruses per cell. At the indicated times, titers of viruses in the cells (A and C) or in the medium (B and D) were determined by plaque assays. For vYFP-A4/ΔA27, titers were determined by counting fluorescent cell foci on the monolayer.

plaques were imaged using a Leica DMIRB inverted fluorescence microscope with a cooled charge-coupled device (Cooke) that was controlled using Image-Pro Plus software (MeidaCybernetics). After imaging, cells were stained with crystal violet, rinsed with water, and air dried. Stained plates were imaged using a Kodak Image Station 2000R (Kodak Digital Science).

Syncytium formation. HeLa cells were infected at a multiplicity of 10. After 15 h the cells were washed with pH 7.4 phosphate-buffered saline and incubated for 2 min in either fusion buffer [10 mM 2-(*N*-morpholino)ethanesolfunic acid and 10 mM HEPES in phosphate-buffered saline at pH 5.5] or control buffer (phosphate-buffered saline, pH 7.4). The buffers were replaced with normal growth medium and incubated for 3 h before imaging with a Leica DMIRB inverted fluorescence microscope.

Virus purification. CsCl purification was carried out as described previously (35). Briefly, monolayers of RK13 cells were infected at a multiplicity of 10. After 2 h, the inoculum was replaced with methionine- and cystein-free growth medium (Cellgro) that contained 2.5% dialyzed fetal bovine serum (Gibco) and 500 μCi of a mixture of [^{35}S]methionine and [^{35}S]cystein (Perkin Elmer). After 18 h of infection, the medium was removed and cells and larger debris were removed by low-speed centrifugation. Cells were dislodged by scraping, collected by low-speed centrifugation, resuspended in swelling buffer (10 mM Tris, pH 10), incubated on ice for 10 min, disrupted by Dounce homogenization, and clarified by low-speed centrifugation. Virus from the cell lysates and from the medium was centrifuged through a 36% sucrose cushion, resuspended in swelling buffer with sonication, and banded on a preformed CsCl step gradient as previously described (12). Gradients were fractionated from the bottom of the tube and the amount of radiation present in each fraction was determined by scintillation counting.

Digital video microscopy. Live cell imaging was carried out essentially as described previously (33, 35, 36). Briefly, HeLa cells were plated at ~80% confluence onto ΔTC3 dishes (Bioptechs, Inc.) and infected the following day with 0.2 PFU of virus per cell. The following day cells were imaged using a Leica DMIRB inverted fluorescence microscope with a cooled charge-coupled device (Cooke) that was controlled using Image-Pro Plus software (MeidaCybernetics). During imaging, cells were maintained at 37°C on a heated ΔTC3 temperature-controlled stage (Bioptechs, Inc.). Virion velocities were calculated using the public domain software NIH Image 1.63 developed at the National Institutes of Health (available at http://rsb.info.nih.gov/nih-image).

For antibody staining, HeLa cells were grown to confluence on coverslips and infected with 1 PFU per cell. The following day, infected cells were fixed with 4% paraformaldehyde and permeabilized with Triton X-100 both in phosphate-buffered saline. To stain the site of wrapping, fixed and permeabilized cells were incubated with anti-B5 monoclonal antibody 19C2 (29) followed by Texas Red-conjugated goat anti-rat antibody (Jackson ImmunoResearch Laboratories). Stained cells on coverslips were mounted in Mowiol containing 1 μg of 4′,6′-diamidino-2-penylindole dihydrochloride (DAPI) (EM Sciences) per ml to visualize DNA in the nucleus and viral factories. Images were collected as described above. The distances between the DAPI-stained factories and the Texas Red-stained site of B5 accumulation were measured using Image-Pro Plus software (MeidaCybernetics). Images were false colored and overlaid using Adobe PhotoShop version 8.

RESULTS

Construction of a recombinant vaccinia virus with a deleted A27L gene. Previous work had indicated that A27 was required

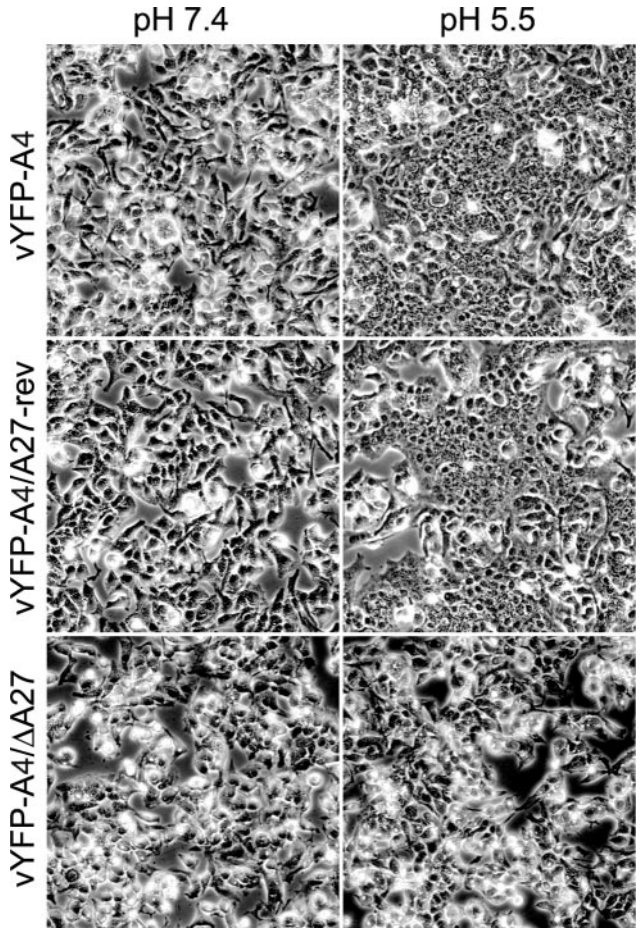

FIG. 3. Induction of syncytia. HeLa cells were infected with the indicated viruses and incubated for 15 h. After incubation, cells were briefly treated with buffer at either pH 7.4 or 5.5, incubated in regular medium for 3 h, and examined by phase-contrast microscopy.

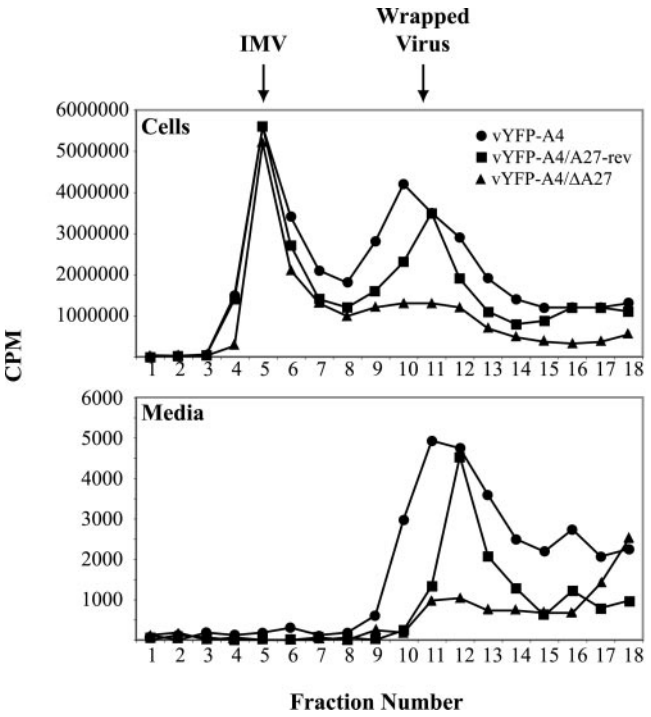

FIG. 4. Isolation of IMV and wrapped viruses. RK13 cells were infected with the indicated viruses at a MOI of 10. Infected cells were labeled with 500 μCi of a mixture of [^{35}S]methionine and [^{35}S]cystein from 4 to 18 h after infection. Particles in the cell lysates and medium were concentrated by sedimentation through a sucrose cushion, applied to a CsCl density gradient, centrifuged, and fractionated. The amount of radioactivity in the fractions was determined by scintillation counting.

for the intracellular movement of IMV (28). We theorized based on the direction of IMV movement away from the viral factory, which is usually located near the nucleus, that A27 would be interacting with the cellular microtubule motor protein kinesin. When a yeast two-hybrid assay failed to detect an interaction between A27 and kinesin, even though a strong interaction was detected between A27 and itself, we decided to investigate further the role of A27 in IMV intracellular movement. It has been reported that a recombinant vaccinia virus, which expressed an A4-green fluorescent protein chimera in place of the normal viral A4 core protein, did not exhibit any defects in infectivity. In addition, the report documented the use of A4-green fluorescent protein to visualize IMV using fluorescence microscopy (5). We decided to start with a similar YFP-A4 recombinant and delete the entire A27L gene using a transient dominant selection scheme along with PCR and sequencing to confirm the removal of the A27L coding sequence. The resulting recombinant virus, vYFP-A4/ΔA27, was unable to form visible plaques on a monolayer of BS-C-1 cells after 4 days. When observed by fluorescent microscopy, individual fluorescent cells were seen, indicating that the virus was infectious but severely diminished in cell-to-cell spread (Fig. 1). To be certain that the defect we observed was not due to disruption of the genes surrounding the removed A27L locus, we constructed a revertant virus that had the A27L gene, under the control of its normal promoter, inserted into the thymidine kinase locus. The revertant (vYFP-A4/A27-rev) formed large plaques similar in size to the parental vYFP-A4, indicating that the small plaque phenotype was due to the removal of the A27L gene (Fig. 1).

Growth properties of recombinant viruses. A recombinant virus containing a total deletion of the A27L gene had not been described previously. Therefore we decided to characterize the growth properties of our novel recombinants starting with a one-step growth curve. Monolayers of BS-C-1 cells were infected with a multiplicity of infection (MOI) of 5 and the amount of virus associated with the cells and released into the media was determined at various times after infection. All three of the viruses produced similar amounts of cell-associated virus (Fig. 2A). Next, the amount of virus released into the media, which is comprised mostly of enveloped virus, was determined. At 48 h postinfection (PI), vYFP-A4 and vYFP-A4/A27-rev showed a 2-log increase when compared to vYFP-A4/ΔA27 (Fig. 2B). Over the entire experiment, vYFP-A4/ΔA27 showed only a slight increase over the 6-h time point that serves as a measure of unbound input virus.

The ability of our recombinants to replicate and spread cell to cell after a low MOI (0.01 PFU/cell) was evaluated over several days. In this assay, vYFP-A4/ΔA27 produced almost 3 logs less virions than both vYFP-A4 and vYFP-A4/A27-rev after 120 h PI (Fig. 2C). This difference was even more pronounced when the amount of virus released into the media was examined. After 120 h PI, vYFP-A4/ΔA27 released almost 4 logs less virus than both vYFP-A4 and vYFP-A4/A27-rev over the same period of time (Fig. 2D). The results from both of these assays indicate that vYFP-A4/ΔA27 is defective in enveloped virus production.

Production of enveloped virions. Cells infected with vaccinia virus can be induced to form syncytia by a brief low-pH treatment at late times of infection due to the deposition of progeny enveloped virions on the cell surface (14). Mutations that inhibit IEV formation will not undergo fusion (2, 10, 37). Based on previous studies (27, 32) and from the results of the growth curves, we predicted that cells infected with vYFP-A4/ΔA27 were not producing IEV and would not undergo syncytium formation after a low-pH treatment. To test this idea cells infected with either vYFP-A4, vYFP-A4/ΔA27, or vYFP-A4/A27-rev were subjected to a brief low-pH treatment and were allowed to recover in normal media for 3 h before being imaged. Cells infected with either vYFP-A4 or vYFP-A4/A27-rev and treated with pH 5.5 buffer formed large syncytia (Fig. 3). In contrast, cells infected with vYFP-A4/ΔA27 failed to form syncytia when treated with pH 5.5 buffer, much like the infected cells treated with pH 7.4 buffer (Fig. 3).

We considered the possibility that vYFP-A4/ΔA27 was forming IEV that were not infectious. Electron microscopic examination of cells infected with vYFP-A4/ΔA27 failed to find wrapped virions either on the cell surface or in the cytoplasm while IMV was seen in abundance, indicating that this was not the case (data not shown). To verify this observation we separated radiolabled lysates from cells infected with the three recombinant viruses using CsCl density gradient to look at wrapped virus (IEV, CEV, and EEV) production. While all three recombinants produced a similar amount of IMV, both vYFP-A4 and vYFP-A4/A27-rev produced significantly greater amounts of wrapped virus than vYFP-A4/ΔA27 that was released into the media and associated with the cell (Fig. 4). All

FIG. 5. Visualization of IMV by digital video microscopy. HeLa cells were infected with 0.2 PFU of vYFP-A4/ΔA27 per cell. Approximately 12 h after infection, images were collected at 1 frame per s. Selected frames are shown with the cumulative time elapsed (in seconds) indicated in the upper left corner. Similar arrows and arrowheads point to the same virion in successive frames. Entire time-lapse videos are available at www.urmc.rochester.edu/GEBS/faculty/brain_ward.htm. Bar, 5 μm.

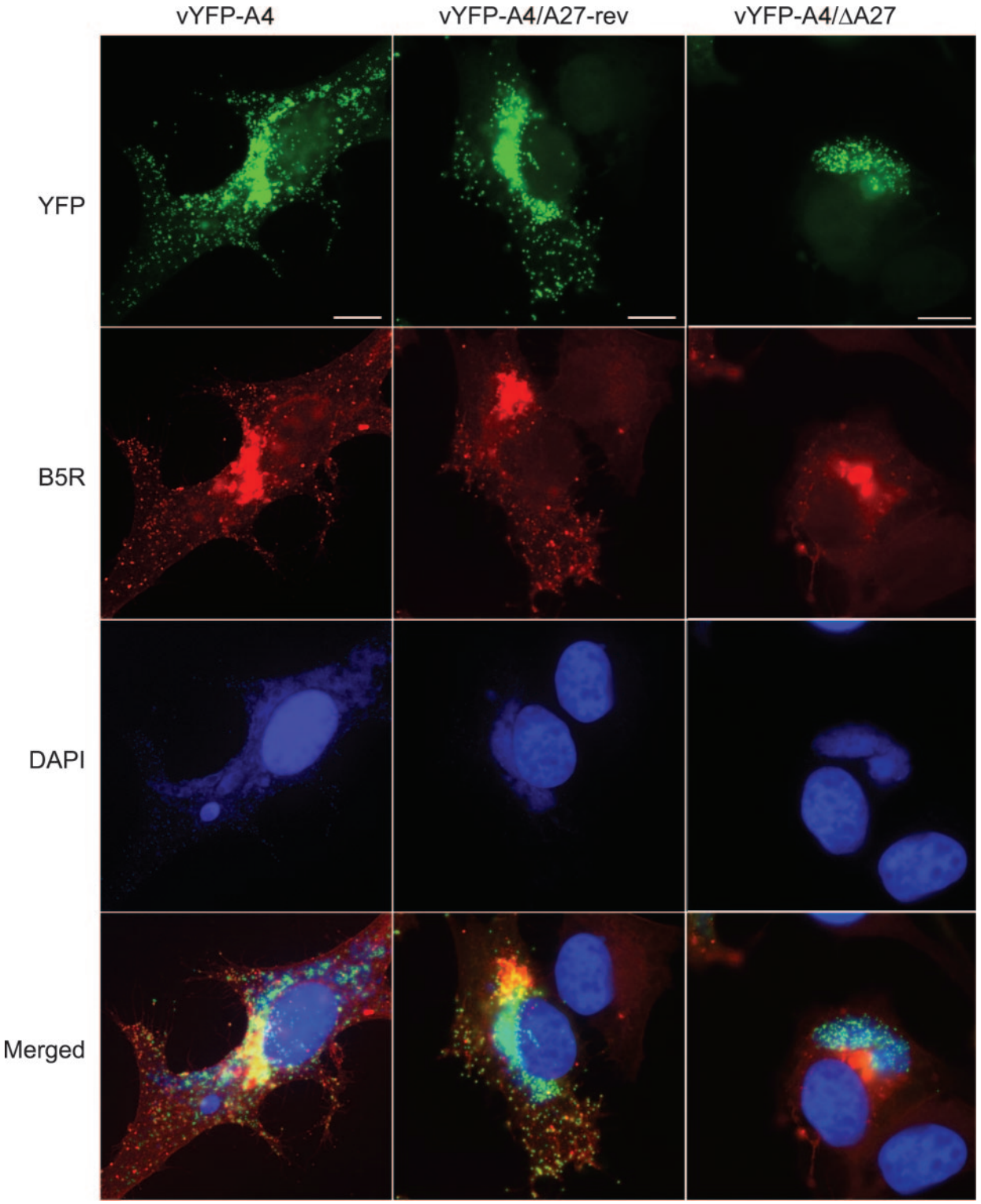

FIG. 6. Localization of viral factories relative to the site of wrapping. HeLa cells were infected with the indicated recombinant viruses and were stained with anti-B5R antiserum followed by Texas Red-conjugated goat anti-rat antibody (red) and DAPI (blue) to visualize DNA. Green fluorescence represents YFP-A4. Bar, 5 μm.

of the preceding assays indicate the vYFP-A4/ΔA27 is severely attenuated in enveloped virus production.

Intracellular movement of YFP-labeled virions. Having established that vYFP-A4/ΔA27 is inhibited in IEV production, we next applied digital video fluorescent microscopy of unfixed cells to assess the role of A27 in IMV intracellular movement. The inability of vYFP-A4/ΔA27 to make IEV simplified the analysis because IEV and IMV are indistinguishable at this

TABLE 1. Frame-by-frame measurements[a] for five individual virions

Frame no.[b]	Virion				
	A	B	C	D	E
1	0.00	0.95	0.67	2.85	1.25
2	0.60	0.27	1.54	0.82	1.03
3	0.00	0.93	0.58	0.20	0.46
4	0.00	0.36	1.21	0.00	1.44
5	0.00	1.49	0.00	0.00	0.30
6	0.00	0.00	0.00	0.00	0.65
7	0.00	0.00	0.00	0.00	0.00
8	0.00	0.00	0.00	0.00	0.00
9	0.00	0.00	0.00	0.00	0.00
10	0.00	0.00	0.00	0.00	0.00
11	0.00	0.00	0.00	0.00	0.00
12	0.87	0.00	0.00	0.00	0.00
13	0.40	0.00	0.53	0.00	0.00
14	0.00	0.00	0.31	0.00	0.00
15	0.00	0.00	0.00	0.00	0.00
16		1.17	0.00	0.00	0.00
17		0.41	0.00	0.00	0.00
18		0.00	0.43	0.00	0.00
19		0.00	0.00	0.00	0.00
20		0.00	0.00	0.00	0.00
21			0.51	0.00	0.00
22			0.00	0.00	0.00
23			0.00	0.00	0.83
24			0.00	0.70	0.00
25				0.00	0.00
Total μm	1.87	5.58	5.78	4.57	5.96
Total s	15	20	24	25	25
Speed (μm/s)	0.12	0.28	0.24	0.18	0.24

[a] Measurements are displayed in μm.
[b] Frame rate equals 1 frame/s.

resolution. HeLa cell monolayers were infected with vYFP-A4/ΔA27, incubated overnight, and live-imaged the next day. At high magnifications a bright fluorescent region that contained individual virion-sized particles could be discerned in a region that correlated with the viral factory (Fig. 5). Despite the absence of A27, virion particles could be discerned moving in the cell (Fig. 5). After transiting away from the factory, many of these particles were seen returning to the factory (representative virions are shown in Fig. 5). As had been shown for intracellular movement of IEV (36), IMV movement was reversibly arrested by application of the microtubule depolymerizing drug nocodazole (data not shown). The speeds for several particles were calculated and five of them are displayed in Table 1. Virion movement reached speeds of 2.8 μm/s and was saltatory in nature with many frames showing no virion movement at all followed by a few frames of rapid movement.

Localization of wrapping. It had been previously reported that a movement defect was at least partially responsible for the inhibited IEV production seen in other A27L mutants (28). To investigate this claim we stained cells infected with vYFP-A4, vYFP-A4/A27-rev, or vYFP-A4/ΔA27 with DAPI to label the viral factory and an antibody that recognizes the envelope-specific protein B5, which would label the site of wrapping. In all cells infected with YFP-A4-containing virus, there was an accumulation of signal over the viral factory. YFP-labeled virions displayed a greater dissemination in cells infected with vYFP-A4 and vYFP-A4/A27-rev. Most of these virions were also stained with anti-B5 antibody, indicating that they were IEV and that the greater dissemination of YFP-labeled virions in these cells was due to the production of wrapped virus (Fig. 6). In a majority of cells, parts of the factory overlapped with or were in close proximity to the site of wrapping labeled by anti-B5 antibody (Fig. 6). To quantitate this observation, the distance between these two sites was measured in 30 cells infected with vYFP-A4/ΔA27. The average distance was determined to be 1.9 μm, well within the distance traveled by the IMV we imaged in the absence of A27. In addition, YFP-labeled virions could be seen in the B5R-labeled area, although we could not determine if they were wrapped IEV or not, in many of the cells infected with vYFP-A4/ΔA27 (Fig. 6; also data not shown), indicating that the absence of A27 did not preclude IMV from traveling to the site of wrapping.

DISCUSSION

The spatial separation between the site of IMV formation in the factory and the site of intracellular envelopment requires the active transport of newly formed IMV to the site of wrapping. We undertook studies to investigate the role of A27 in IMV movement. After a yeast two-hybrid assay failed to detect an interaction between A27 and kinesin, we decided to directly assess the role of A27 in IMV movement by constructing a recombinant virus that had the gene deleted. The recombinant, vYFP-A4/ΔA27 was severely attenuated in the production of IEV but not IMV. Because IEV and IMV are indistinguishable at this resolution, the inability of vYFP-A4/ΔA27 to make IEV simplified our analysis. Live examination of cells infected with the recombinant revealed a bright fluorescent signal over the viral factory that contained individual virion-sized particles. The majority of virions were stationary but some individual virions could be visualized moving out away from the factory at speeds approaching 3 μm/s. The movement appeared bidirectional with many of the virions returning to the factory region after initially moving away. We were unable to discern any movement in cells that were infected in the presence of the vaccinia virus morphogenesis blocking drug rifampin, indicating that movement was specific to virion formation (data not shown). The maximal speeds observed for IMV movement are consistent with the maximal speed of 2.7 μm/s observed for post-Golgi transport vesicles that utilize microtubules (17). In addition, IMV movement was reversibly arrested in the presence of the microtubule depolymerizing drug nocodazole (data not shown), consistent with IMV movement in the absence of A27 being microtubule based.

Past studies of A27 utilized viruses that had either mutated forms or inducible expression of A27 (9, 14, 27, 28, 32) presumably due to the difficulty in isolating and purifying a virus containing an A27L deletion. We chose not to use these viruses because we feared that conducting our experiments in the presence of either a mutated form of A27 or low levels of full-length A27, due to leakiness of inducible systems (27, 32), would complicate the analysis of IMV movement. The inability to isolate a ΔA27L virus may be explained by the severe attenuation in IEV production and subsequent miniscule plaque formation by vYFP-A4/ΔA27. The one to three cell plaques formed by vYFP-A4/ΔA27, even after 4 days, are virtually

undetectable using light microscopy (Fig. 1) and therefore would be almost impossible to isolate. We were able to visualize these few infected cells because they fluoresced due to the expression of YFP-A4. This visualization made it possible to pick cells infected with vYFP-A4/ΔA27 and propagate the recombinant even though it was inhibited in IEV production.

Previous reports have established the dependence of IEV on microtubules for transport to the cell surface (13, 18, 23, 34–36). Indeed, a direct link between IEV and the kinesin light chain through the viral A36 protein was recently reported (34). Although IMV and IEV intracellular movement are similar in that they are saltatory, sensitive to nocodazole, and appear to be capable of bidirectional movement, they differ in a distinct way. The movement of IMV is much shorter, traveling only a few microns before stopping for very long periods of time. This difference indicates that whichever protein provides the tether for IMV, it most likely has a lower affinity for kinesin than the IEV-specific protein A36, which links IEV with kinesin (34). This lowered affinity would result in both longer lag times between IMV movements and shorter interaction times. The need for bidirectional IMV movement is unclear. One possibility is that bidirectional movement is involved in limiting the number of IMVs that become enveloped by concentrating them through a retrieval mechanism in the factory region. Furthermore, our observation that only a minority of IMVs are seen moving is consistent with the relatively small number of IMVs that proceed on to become IEV and once again suggests that IMV movement may be a determining factor in the progression of IMV to IEV. Further experiments will be required to discern the role of IMV movement during morphogenesis.

A previous report indicated that A27 was required for IMV movement based on data that showed virions were less distributed throughout the cytoplasm of infected cells when A27 expression was repressed (28). Our results offer an alternative explanation. Due to the ability to move bidirectionally on microtubules, IMVs simply return to the viral factory in the absence of A27 and envelopment. It should be noted that our results do not exclude a role for A27 in the transport of IMV. They only indicate that A27 is not required and it is possible that a separate A27-dependent pathway exists. Furthermore, we have shown that in the absence of A27, IMV can still be transported distances sufficient to reach the site of wrapping, indicating that the only defect of a virus with a deletion of A27L is an inability to produce enveloped virus.

ACKNOWLEDGMENTS

I thank Bernie Moss and Tatiana Senkevich for providing the parent vA-4YFP virus, Dennis McCance for critical reading of the manuscript, Karen Bentley for electron microscopy, and Kathleen Gillespie for maintenance of cell lines.

This work was supported by grant AI54392 from the National Institutes of Health.

REFERENCES

1. **Appleyard, G., A. J. Hapel, and E. A. Boulter.** 1971. An antigenic difference between intracellular and extracellular rabbitpox virus. J. Gen. Virol. **13:**9–17.
2. **Blasco, R., and B. Moss.** 1991. Extracellular vaccinia virus formation and cell-to-cell virus transmission are prevented by deletion of the gene encoding the 37,000-dalton outer envelope protein. J. Virol. **65:**5910–5920.
3. **Blasco, R., and B. Moss.** 1992. Role of cell-associated enveloped vaccinia virus in cell-to-cell spread. J. Virol. **66:**4170–4179.
4. **Boulter, E. A., and G. Appleyard.** 1973. Differences between extracellular and intracellular forms of poxvirus and their implications. Prog. Med. Virol. **16:**86–108.
5. **Carter, G. C., G. Rodger, B. J. Murphy, M. Law, O. Krauss, M. Hollinshead, and G. L. Smith.** 2003. Vaccinia virus cores are transported on microtubules. J. Gen. Virol. **84:**2443–2458.
6. **Chung, C.-S., J.-C. Hsiao, Y.-S. Chang, and W. Chang.** 1998. A27L protein mediates vaccinia virus interaction with cell surface heparin sulfate. J. Virol. **72:**1577–1585.
7. **Cudmore, S., I. Reckmann, G. Griffiths, and M. Way.** 1996. Vaccinia virus: a model system for actin-membrane interactions. J. Cell Sci. **109:**1739–1747.
8. **Dales, S., and L. Siminovitch.** 1961. The development of vaccinia virus in Earle's L strain cells as examined by electron microscopy. J. Biophys. Biochem. Cytol. **10:**475–503.
9. **Dallo, S., J. F. Rodriguez, and M. Esteban.** 1987. A 14K envelope protein of vaccinia virus with an important role in virus-host cell interactions is altered during virus persistence and determines the plaque size phenotype of the virus. Virology **159:**423–432.
10. **Doms, R. W., R. Blumenthal, and B. Moss.** 1990. Fusion of intra- and extracellular forms of vaccinia virus with the cell membrane. J. Virol. **64:**4884–4892.
11. **Earl, P. L., and B. Moss.** 1991. Generation of recombinant vaccinia viruses, p. 16.17.1–16.17.16. *In* F. M. Ausubel, R. Brent, R. E. Kingston, D. D. Moore, J. G. Seidman, J. A. Smith, and K. Struhl (ed.), Current protocols in molecular biology, vol. 2. Greene Publishing Associates and Wiley Interscience, New York, N.Y.
12. **Engelstad, M., and G. L. Smith.** 1993. The vaccinia virus 42-kDa envelope protein is required for the envelopment and egress of extracellular virus and for virus virulence. Virology **194:**627–637.
13. **Geada, M. M., I. Galindo, M. M. Lorenzo, B. Perdiguero, and R. Blasco.** 2001. Movements of vaccinia virus intracellular enveloped virions with GFP tagged to the F13L envelope protein. J. Gen. Virol. **82:**2747–2760.
14. **Gong, S. C., C. F. Lai, and M. Esteban.** 1990. Vaccinia virus induces cell fusion at acid pH and this activity is mediated by the N-terminus of the 14-kDa virus envelope protein. Virology **178:**81–91.
15. **Grimley, P. M., E. N. Rosenblum, S. J. Mims, and B. Moss.** 1970. Interruption by rifampin of an early stage in vaccinia virus morphogenesis: accumulation of membranes which are precursors of virus envelopes. J. Virol. **6:**519–533.
16. **Hiller, G., K. Weber, L. Schneider, C. Parajsz, and C. Jungwirth.** 1979. Interaction of assembled progeny pox viruses with the cellular cytoskeleton. Virology **98:**142–153.
17. **Hirschberg, K., C. M. Miller, J. Ellenberg, J. F. Presley, E. D. Siggia, R. D. Phair, and J. Lippincott-Schwartz.** 1998. Kinetic analysis of secretory protein traffic and characterization of golgi to plasma membrane transport intermediates in living cells. J. Cell Biol. **143:**1485–1503.
18. **Hollinshead, M., G. Rodger, H. Van Eijl, M. Law, R. Hollinshead, D. J. Vaux, and G. L. Smith.** 2001. Vaccinia virus utilizes microtubules for movement to the cell surface. J. Cell Biol. **154:**389–402.
19. **Lai, C. F., S. C. Gong, and M. Esteban.** 1991. The purified 14-kilodalton envelope protein of vaccinia virus produced in *Escherichia coli* induces virus immunity in animals. J. Virol. **65:**5631–5635.
20. **Lai, C. F., S. C. Gong, and M. Esteban.** 1990. Structural and functional properties of the 14-kDa envelope protein of vaccinia virus synthesized in Escherichia coli. J. Biol. Chem. **265:**22174–22180.
21. **Moss, B.** 2001. *Poxviridae*: the viruses and their replication, p. 2849–2883. *In* B. N. Fields, D. M. Knipe, and P. M. Howley (ed.), Fields virology, 4th ed., vol. 2. Lippincott-Raven Publishers, Philadelphia, Pa.
22. **Payne, L. G.** 1980. Significance of extracellular enveloped virus in the in vitro and in vivo dissemination of vaccinia. J. Gen. Virol. **50:**89–100.
23. **Rietdorf, J., A. Ploubidou, I. Reckmann, A. Holmstrom, F. Frischknecht, M. Zettl, T. Zimmermann, and M. Way.** 2001. Kinesin-dependent movement on microtubules precedes actin-based motility of vaccinia virus. Nat. Cell Biol. **3:**992–1000.
24. **Rodriguez, D., J. R. Rodriguez, and M. Esteban.** 1993. The vaccinia virus 14-kilodalton fusion protein forms a stable complex with the processed protein encoded by the vaccinia virus A17L gene. J. Virol. **67:**3435–3440.
25. **Rodriguez, J. F., R. Janeczko, and M. Esteban.** 1985. Isolation and characterization of neutralizing monoclonal antibodies to vaccinia virus. J. Virol. **56:**482–488.
26. **Rodriguez, J. F., E. Paez, and M. Esteban.** 1987. A 14,000-Mr envelope protein of vaccinia virus is involved in cell fusion and forms covalently linked trimers. J. Virol. **61:**395–404.
27. **Rodriguez, J. F., and G. L. Smith.** 1990. IPTG-dependent vaccinia virus: identification of a virus protein enabling virion envelopment by Golgi membrane and egress. Nucleic Acids Res. **18:**5347–5351.
28. **Sanderson, C. M., M. Hollinshead, and G. L. Smith.** 2000. The vaccinia virus A27L protein is needed for the microtubule-dependent transport of intracellular mature virus particles. J. Gen. Virol. **81:**47–58.
29. **Schmelz, M., B. Sodeik, M. Ericsson, E. J. Wolffe, H. Shida, G. Hiller, and G. Griffiths.** 1994. Assembly of vaccinia virus: the second wrapping cisterna is derived from the trans Golgi network. J. Virol. **68:**130–147.
30. **Stokes, G. V.** 1976. High-voltage electron microscope study of the release of vaccinia virus from whole cells. J. Virol. **18:**636–643.
31. **Tooze, J., M. Hollinshead, B. Reis, K. Radsak, and H. Kern.** 1993. Progeny

vaccinia and human cytomegalovirus particles utilize early endosomal cisternae for their envelopes. Eur. J. Cell Biol. **60:**163–178.
32. **Vazquez, M. I., and M. Esteban.** 1999. Identification of functional domains in the 14-kilodalton envelope protein (A27L) of vaccinia virus. J. Virol. **73:**9098–9109.
33. **Ward, B. M.** 2004. Pox, dyes, and videotape: making movies of GFP-labeled vaccinia virus. Methods Mol. Biol. **269:**205–218.
34. **Ward, B. M., and B. Moss.** 2004. Vaccinia virus A36R membrane protein provides a direct link between intracellular enveloped virions and the microtubule motor kinesin. J. Virol. **78:**2486–2493.
35. **Ward, B. M., and B. Moss.** 2001. Vaccinia virus intracellular movement is associated with microtubules and independent of actin tails. J. Virol. **75:** 11651–11663.
36. **Ward, B. M., and B. Moss.** 2001. Visualization of intracellular movement of vaccinia virus virions containing a green fluorescent protein-B5R membrane protein chimera. J. Virol. **75:**4802–4813.
37. **Wolffe, E. J., S. N. Isaacs, and B. Moss.** 1993. Deletion of the vaccinia virus B5R gene encoding a 42-kilodalton membrane glycoprotein inhibits extracellular virus envelope formation and dissemination. J. Virol. **67:**4732–4741. (Erratum, **67:**5709–5711.)